Published in final edited form as:
Toxicology. 2008 April 18; 246(2-3): 172–179. doi:10.1016/j.tox.2008.01.008.

Autoantibodies from mice exposed to Libby amphibole asbestos bind SSA/Ro52 – enriched apoptotic blebs of murine macrophages

David J. Blake[*], **Scott A. Wetzel**[*], and **Jean C. Pfau**[†]

[*]*Division of Biological Sciences, University of Montana, Missoula, Montana, 59812*

[†]*Department of Biomedical & Pharmaceutical Sciences, Center for Environmental Health Sciences, University of Montana, Missoula, Montana, 59812*

Abstract

Asbestos exposure is associated with increased autoimmune responses in humans. For example, in Libby, MT where significant asbestos exposure has occurred due to an asbestos contaminated vermiculite mine near the community, residents have developed increased autoimmune responses compared to an unexposed population. However, the exact mechanism by which Libby amphibole asbestos generates autoimmune responses is unclear. A murine model of amphibole asbestos-induced autoimmunity was recently established, and one of the targets of the autoantibodies was the SSA/Ro52 autoantigen. The purpose of this study was to determine whether the SSA/Ro52 autoantigen is exposed at the surface of cells as a result of asbestos exposure as a possible mechanism leading to antigenicity. Our results indicate that Libby asbestos induces apoptosis in murine macrophages as determined by phosphatidylserine exposure, cleavage of poly (ADP-ribose) polymerase and morphological changes such as nuclear condensation. Moreover, asbestos induced apoptosis results in the formation of apoptotic cell surface blebs enriched in SSA/Ro52 as determined by confocal microscopy. Most importantly, apoptotic cell surface blebs are recognized by autoantibodies from mice exposed to amphibole asbestos suggesting that these cell surface structures may be antigenic when presented in a pro-inflammatory context. This study supports the hypothesis that the induction of apoptosis plays a key role in environmentally-induced autoimmunity through cell surface exposure of a known autoantigen.

Keywords

asbestos; macrophage; apoptosis; autoimmunity; immunotoxicology

Introduction

Systemic autoimmune disease (SAID), such as rheumatoid arthritis, systemic lupus erythematosus and scleroderma, occurs when self-reactive T and B cells escape the protective tolerizing safe guards of the immune system and cause tissue damage, resulting in a diversity

Corresponding Author Mailing Address: Johns Hopkins School of Environmental Health, Johns Hopkins University, 615 N. Wolfe St., Baltimore, MD 21205, Phone: (410) 502-9120. Email: dblake@jhsph.edu.

of debilitating symptoms. Although it is widely accepted that environmental factors combine with genetic susceptibility to exacerbate the development of these diseases, critical knowledge gaps remain regarding the mechanisms involved. The association of SAID with exposure to inhaled environmental silicates, asbestos and silica, provides an important experimental framework needed to fill those gaps.

Exposure to environmental xenobiotics such as silica, mercury and vinyl chloride is associated with the production of autoantibodies (AAs) and the development of systemic autoimmune disease (D'Cruz 2000; Hess 2002; Parks and Cooper 2005). Increased serum immunoglobulins, positive anti-nuclear autoantibody (ANA) tests and immune complexes have also been reported in small cohorts of individuals exposed to asbestos, a naturally occurring crystalline silicate fiber. The ability of asbestos exposure to exacerbate autoimmune responses in humans is supported by studies of an asbestos-exposed population from Libby, MT. Residents of Libby have higher frequencies and titers of positive ANA tests compared to an unexposed control population (Pfau et al. 2005), as well as increased risk for SAID, which is dependent upon the routes of exposure (Noonan et al. 2006). Although the exact mechanisms that lead to the induction of SAID and AA production as a result of environmental exposure have not been established, evidence supports the role of apoptosis as a potential initiating stimulus (Casciola-Rosen *et al.* 1994; Rosen and Casciola-Rosen 1999, 2004). Considerable literature supporting a role for apoptosis in silica-induced autoimmunity was recently reviewed (Brown 2004), emphasizing the ability of silica to induce apoptosis and to drive SAID. Because asbestos can also cause apoptosis (Hamilton et al. 1996), a similar mechanism may link asbestos with systemic autoimmune responses.

Therefore, a murine model of asbestos-induced autoimmunity was recently established (Pfau et al. In Press). Asbestos exposed mice develop positive antinuclear antibody tests and mild glomerulonephritis suggestive of a systemic lupus erythematosus (SLE)-like disease. The asbestos induced SLE-like disease is characterized by the production of AAs that recognize the SSA/Ro52 autoantigen. SSA/Ro52 is a newly characterized RING-finger-type E3 ubiquitin ligase (Espinosa *et al.* 2006; Wada and Kamitani 2006), which in unstimulated cells localizes to the cytoplasm (Ohlsson et al. 2002). Autoantibodies against SSA/Ro52 are commonly found in patients with SLE (Hassan *et al.* 2002; Hoffman *et al.* 2004; Popovic *et al.* 2007; Routsias *et al.* 2006). Interestingly, SSA/Ro52 redistributes itself to apoptotic blebs in cardiac monocytes, epithelial cells, salivary gland cells and keratinocytes after exposure to various pro-apoptotic agents (Igarashi *et al.* 1995; McArthur *et al.* 2002; Miranda *et al.* 1998; Ohlsson *et al.* 2002). Because AAs target SSA/Ro52 during autoimmune responses, the clustering of SSA/Ro52 to small surface blebs of apoptotic cells may be important in the induction of autoimmunity generated by xenobiotics (Casciola-Rosen et al. 1994).

Alveolar macrophages are the primary cells that interact with inhaled particles and function to clear particles from the lung. Our study utilizes RAW264.7 cells, a phagocytic murine cell line with characteristics similar to alveolar macrophages (Xia et al. 2006). We have previously shown that exposure to Libby amphibole asbestos induces oxidative stress in these cells (Blake et al. 2007). The results of this study extend these findings and indicate that Libby asbestos induces apoptosis in macrophages leading to the redistribution of SSA/Ro52 to apoptotic blebs. The fact that antibodies from asbestos-exposed mice recognize these surface blebs suggests that the antigen in the apoptotic blebs can be immunogenic *in vivo*, ultimately resulting in production of autoantibodies. This model has great potential to a) clearly establish direct evidence for a role of apoptosis in silicate-induced autoimmunity, including mechanisms of lost tolerance to apoptotic material, b) explore anti-Ro52 as a possible early marker of developing SAID following exposures, and c) reveal potential therapeutic targets to halt disease progression.

Materials and Methods

Cell culture conditions

Mouse macrophages, RAW264.7 cells, (ATCC-2091: American Type Culture Collection, Manassas, VA) were cultured at 37°C in a 5% CO_2 incubator in complete media, which contained DMEM media with 4.5 g/L glucose and L-glutamine supplemented with 1.5 mM sodium pyruvate, 20 mM HEPES, 55 μM 2-mercaptoethanol, 10% fetal bovine serum and antibiotics (100 U/ml penicillin, 100 μg/ml streptomycin and 0.25 μg/ml amphotericin B) (Gibco BRL, Bethesda, MD). Confluent RAW264.7 cells were scraped from T75 flasks, counted with a Z series Coulter Counter (Beckman Coulter, Hialeah, FL) and plated into 12 well plates, 8-well chambered coverslips (Nalge Nunc International Corp., Rochester, NY) or T75 flasks in complete media and allowed to adhere overnight prior to exposure to asbestos fibers.

Particulate Matter

Libby asbestos was kindly provided by the US Geological Survey. The Libby amphibole fibers have been chemically and physically characterized in detail and contain amphibole fibers from six locations at the vermiculite mine, including winchite, richterite and tremolite (Wylie et al. 2000; Gunter et al. 2003; Meeker et al. 2003). Therefore, the asbestos sample is labeled in this paper as Libby 6-mix. Korean tremolite for the mouse studies was obtained from National Institute of Standards and Technology (NIST). Wollastonite, a non-cytotoxic, non-fibrogenic control fiber, was provided by NYCO Minerals (Willsboro, NY). Fibers were dispersed in phosphate buffered saline (PBS) (pH 7.4) by cup-horn sonication (Misonix, Framingdale, NY) before culturing. Stock concentration suspensions of fibers were prepared fresh immediately prior to their addition into DMEM cell cultures. Fiber concentrations were based on relative mass.

The presence of lipopolysaccharide (LPS) in the Libby 6-mix sample was quantified using the PyroGene Recombinant Factor C Endotoxin Detection System (Cambrex BioScience, Walkersville MD). The limit of detection of the assay is 0.01 EU/ml with 12 EU approximately equal to 1 ng. Therefore, below detectable limits equals less than 1 pg/ml of LPS. LPS contamination of the Libby 6-mix asbestos fibers was tested at 62.5 ug/cm^2 and up to 625 ug/cm^2. All concentrations tested were below the limit of detection, therefore, we conclude that the Libby 6-mix asbestos is free of LPS contamination.

Detection and quantification of apoptosis

RAW264.7 cells were exposed to a final fiber concentration of 62.5 ug/cm^2 for up to 72 h. In control samples, apoptosis was induced by incubation with 1 μM staurosporine (Sigma-Aldrich, St. Louis, MO) for 6 hours (Yamaki et al. 2002). Apoptosis was quantified using APC-conjugated Annexin V (BD Bioscience, San Jose, CA) according to manufacturer's instructions and modified as described earlier (van Engeland et al. 1996). Briefly, cells were exposed to fibers, rinsed with PBS, and incubated in binding buffer containing 0.01 M Hepes (pH 7.4), 0.14 M NaCl and 2.5 mM $CaCl_2$. Staining was performed according to the protocol provided by the manufacturer. Cells were washed then transferred to filter-top polypropylene tubes (BD Labware, Franklin Lanes, NJ) for analysis. Data analysis was performed using FACSDiva software (BD Biosciences) for far red fluorescence. Apoptosis was also detected through immunoblotting with an anti-Poly (ADP-ribose) polymerase (PARP) rabbit polyclonal antibody (Biomol, Plymouth Meeting, PA) as described below, to demonstrate PARP cleavage.

Immunoblotting

Cells were lysed in RIPA buffer (50 mM Tris-HCl (pH 7.4), 150 mM NaCl, 1 mM EDTA, 1% Triton, 1% Sodium deoxycholate, 0.1% SDS, complete protease-inhibitor cocktail (Roche, Indianapolis, IN). Cell lysates were sonicated and the total protein content was determined by the bicinchoninic acid (BCA) protein assay (Pierce, Rockford, IL). Equal amounts of total protein (50 μg) were resolved by SDS-PAGE and were transferred to nitrocellulose membranes (Millipore, Marlborough, MA). Non-specific binding sites were blocked by incubation for 1 h at room temperature with PBS containing 0.05% Tween-20 (PBST) and 5% non-fat dry milk. Membranes were exposed to either a rabbit anti-SSA/Ro52 polyclonal antibody (Chemicon International, Temecula, CA), a mouse anti-actin monoclonal antibody (Abcam, Cambridge, MA), a rabbit anti-PARP polyclonal antibody (Biomol) or whole mouse sera in PBST-0.5% milk overnight at 4°C followed by incubation with horseradish peroxidase-conjugated secondary antibodies (Jackson ImmunoResearch, West Grove, PA). Immunoreactivity was visualized by chemiluminescence substrate according to the manufacturer's instructions (Pierce) and was quantified by densitometry using a FujiReader LAS-3000 (Fujifilm, Stamford, CT).

Immunofluorescence

Cells were plated in 8-well chambered coverslips and exposed to asbestos fibers. After 48 h, cultures were washed in PBS and fixed with 2% formaldehyde and 0.5% glutaraldehyde for 1 h at 4°C. Following washing, cells were blocked in buffer containing 4% normal goat serum, 0.1% bovine serum albumin and 0.1% sodium azide for 1 h at room temperature. SSA/Ro-52 was detected using a rabbit anti-SSA/Ro52 polyclonal antibody (Chemicon) and an Alexa Fluor 488-conjugated goat anti-rabbit antibody (Molecular Probes, Eugene, OR) in blocking buffer. Bound autoantibodies from asbestos exposed mice were detected using an Alexa Fluor 647-conjugated goat anti-mouse IgG antibody (Molecular Probes). The plasma membrane was visualized using Alexa Fluor 647 cholera toxin subunit B conjugate (Molecular Probes). The nucleus was visualized with propidium iodide (PI) after treatment with RNase A (Roche, Indianapolis, IN). Chambers were mounted with FluorSave Reagent (EMD Biosciences, San Diego, CA) and visualized using an inverted Nikon TE-300 microscope. Fluorescence was examined with a 1.4 NA 60X lens using a Bio-Rad Radiance 2000 laser scanning confocal microscope. Channels were recorded sequentially using 488 nm excitation and 515/30 nm emission for Alexa Fluor 488, 543 nm excitation and 600/50 nm emission for PI, and 637 nm excitation and 660 LP for Alexa Fluor 647. Images were collected using Kalman method and merged using Lasersharp software (Bio-Rad, Hercules, CA). 50 cells were visualized for each experiment. All experiments were performed independently at least twice, with similar results.

Colocalization analysis

Confocal microscopy images were analyzed for colocalization of SSA/Ro52 proteins with the purified rabbit anti-SSA/Ro52 polyclonal antibody and sera from asbestos-instilled mice by use of ImageJ (National Institutes of Health, Bethesda, MD) using Just Another Co-localization plugin (JACoP) (Bolte and Cordelieres 2006). Three separate methods were used to calculate Pearson’s correlation coefficient, which measures the extent of colocalization. Pearson's correlation coefficient can range from +1 for complete correlation to −1 for complete exclusion of two fluorophores. Pearson's correlation coefficient was determined as described by Manders (Manders et al. 1993) using Costes’ automatic threshold and Costes’ randomization based colocalization, using 200 randomizations per image (Costes et al. 2004). Colocalization was considered significant if all three coefficients were greater than 0.6.

Mice

Eight week old C57Bl/6 mice (Jackson Laboratories, Bar Harbor, ME) were housed under specific pathogen-free conditions with a 12-hour light and 12-hour dark cycle, constant temperature, and free access to food and water. Euthanasia was performed by ip injection of a lethal dose of sodium pentobarbital, consistent with the recommendations of the Panel on Euthanasia of the American Veterinary Medical Association. All protocols for the use of animals were approved by the University of Montana Institutional Animal Care and Use Committee (IACUC).

Asbestos instillation

C57Bl/6 mice were instilled intra-tracheally with saline, wollastonite or Korean tremolite with a total of two doses, each dose being 60 μg of the fibers sonicated in sterile PBS, given one week apart in the first two weeks of the 7 month experiment as previously described (Pfau et al. In Press). Briefly, suspensions of 30 μl were injected into the trachea via 25 gauge needles, and the incision was closed with 3M Vetbond tissue adhesive. The animals were monitored biweekly for autoantibody production. Blood samples were obtained through saphenous vein bleeds, and then by cardiac puncture after euthanization at 7 months after instillation. Serum was collected from the blood by centrifugation following clotting at room temperature. Serum samples were stored at −20°C until analysis.

Detection of autoantibodies

Specific autoimmune targets were identified by immunoblotting on nitrocellulose bound with known nuclear antigens (MarDx Marblot, SLR Research, Carlsbad, CA), according to the manufacturer's instructions, modified to detect mouse IgG using a goat anti-mouse IgG secondary antibody conjugated to alkaline phosphatase (SouthernBiotech, Birmingham AL). Reactivity of murine autoantibodies against SSA/Ro52 was confirmed by an SSA ELISA kit (INOVA Diagnostics, San Diego, CA) modified to detect mouse IgG using goat anti-mouse secondary antibody (Jackson ImmunoResearch, Philadelphia PA).

Statistical Analysis

Data are given as mean ± standard error of the mean (SEM). Analyses were done using GraphPad Prism 3.03 (GraphPad, San Diego, CA) One-way analysis of variance (ANOVA) was used to compare groups with one variable. A Bonferroni post test was used to compare different treatments. Statistical significance was established as a two-tailed probability of type I error occurring at less than 5%.

Results

Libby 6-mix induces apoptosis in murine macrophages

We have previously reported that Libby 6-mix asbestos decreases cell viability in RAW264.7 cells after 24 h at a final concentration of 62.5 μg/cm^2 (Blake et al. 2007). To determine whether the decrease in cell viability was a result of apoptosis, RAW264.7 cells were exposed to Libby 6-mix as previously described (Blake et al. 2007) and apoptosis was quantified through Annexin V staining. Untreated control cells maintained a basal level of apoptosis of 3 to 5 percent (Fig. 1). Exposure to Libby 6-mix asbestos significantly increased the number of apoptotic cells to 10 percent after 24 h and 20 percent after 48 h compared to untreated control cells ($P < 0.05$). The increase in apoptosis remained stable after 72 h of asbestos exposure (data not shown). After 6 hours of staurosporine treatment greater than 50 percent of macrophages were apoptotic. Exposure to 1 μM staurosporine was used as a positive control to stimulate apoptosis. In contrast, exposure to wollastonite fibers, which is a non-cytotoxic control fiber,

did not induce apoptosis in macrophages. These results indicate that Libby 6-mix asbestos induces apoptosis in murine macrophages.

A second indicator of apoptosis is the cleavage of a select group of nuclear proteins (Casiano et al. 1996). Poly (ADP-ribose) polymerase (PARP) is a 116 kDa nuclear protein that is cleaved into an 89 and 24 kDa fragment during apoptosis (Duriez and Shah 1997). Therefore, to confirm that exposure to Libby 6-mix triggers apoptosis in macrophages, RAW264.7 cells were exposed to Libby 6-mix for up to 72 h. Total cell lysates were prepared and analyzed through immunoblotting. In untreated RAW264.7 cells, PARP existed primarily as a 116 kDa protein. Treatment of macrophages with 1 μM staurosporine for 6 hours resulted in the cleavage of the full length PARP protein into the 89 kDa fragment, which is consistent with previous results (Fig. 2A) (Yamaki et al. 2002). Exposure to Libby 6-mix resulted in a reduction of full length PARP protein compared to the total amount of protein as quantified by densitometry after 24 h (Fig 2B). The reduction of full length protein was associated with an increase in the amount of the 89 kDa fragment after 72 h. Together these data confirm that Libby 6-mix induces apoptosis in murine macrophages.

Although PARP is cleaved during apoptosis, previous results have indicated that the SSA/Ro52 autoantigen is not cleaved during Fas-mediated apoptosis in T cells (Casiano et al. 1996). However, we deemed it necessary to confirm these results for two reasons. First, since this study focuses on a different cell type and apoptotic inducing stimulus, we wanted to make certain that SSA/Ro52 was not cleaved in response to Libby asbestos in macrophages. Second, for subsequent confocal microscopy studies using commercially available antibodies as well as AAs from asbestos exposed mice, it was necessary to ensure that the full length protein remained uncleaved during apoptosis. Consequently, RAW264.7 cells were exposed to Libby 6-mix for 72 h and potential cleavage fragments of SSA/Ro52 were analyzed through immunoblotting. As seen in Figure 3, no cleavage of the SSA/Ro52 autoantigen was evident after 72 h of Libby 6-mix exposure or with staurosporine treatment. These results confirm that SSA/Ro52 is not cleaved during apoptosis and supports previously published results (Casiano et al. 1996).

SSA/Ro52 redistributes to apoptotic blebs as a result of exposure to Libby 6-mix

To determine whether SSA/Ro52 localizes to cell surface blebs during asbestos-induced apoptosis, murine macrophages were exposed to Libby 6-mix and the localization of SSA/Ro52 was determined by confocal microscopy. Murine macrophages were fixed and immunochemically stained using an anti-SSA/Ro52 rabbit polyclonal antibody and an Alexa Fluor 488-conjugated secondary antibody (Green in Fig. 4A, E and I). Nuclei (DNA) were visualized with propidium iodide (PI) (Red in Fig. 4B, F and J). The plasma membrane was visualized by using an Alexa Fluor 647 cholera toxin subunit B conjugate (Magenta in Fig. 4C, G and K).

In normal, unstimulated macrophages, SSA/Ro52 localized to the cytoplasm of cells as shown in the top row (Figure 4D). However, asbestos exposure resulted in the redistribution of SSA/Ro52 to surface blebs of apoptotic cells. The bottom 2 rows show representative cells identified as apoptotic by morphological changes evident in the nucleus, such as elongation, condensation or fragmentation (Arrows, Fig 4F and J) as previously described (Nozawa et al. 2002). Apoptotic blebs enriched in the SSA/Ro52 autoantigen were seen at the surface of apoptotic cells and were compartmentalized within membrane bound structures (Arrow, Fig. 4H). Compartmentalization of SSA/Ro52 to membrane bound structures was confirmed through Z-stack image analysis (data not shown). Apoptotic cells in a more advanced stage of apoptosis also underwent apoptotic membrane blebbing at their surface (Arrow, Fig. 4L). Generally, larger apoptotic blebs contained SSA/Ro52 and DNA whereas smaller apoptotic blebs contained high concentrations of SSA/Ro52 and lacked nuclear material. Greater than 60% of

cells showing morphological changes in the nucleus, suggestive of apoptosis, also showed colocalization of SSA/Ro52 to membrane blebs. The translocation of SSA/Ro52 to membrane blebs during apoptosis was confirmed in RAW264.7 cells with 1 μM staurosporine treatment (Arrow, Fig. 5D). These results confirm that SSA/Ro52 does redistribute to surface blebs of apoptotic cells after exposure to Libby amphibole asbestos.

Apoptotic blebs containing SSA/Ro52 are recognized by autoantibodies from asbestos-exposed mice

To determine whether AAs from asbestos-instilled mice target SSA/Ro52 on the surface of apoptotic cells, murine macrophages were exposed to Libby asbestos as described above, fixed and immunochemically stained using an anti-SSA/Ro52 rabbit polyclonal antibody and an Alexa Fluor 488-conjugated secondary antibody (Green in Fig. 6). Nuclei were visualized with PI (Cyan in Fig. 6). Autoantigens targeted by mouse sera from asbestos-instilled or control mice were visualized with an Alexa Fluor 647-conjugated secondary antibody (Red in Fig. 6). Sera from mice exposed to tremolite asbestos (a component of Libby 6-mix) have been shown to be positive for anti-SSA/Ro52 autoantibodies through ELISA and immunoblotting (Pfau et al. In Press). In contrast, sera from PBS or wollastonite-treated animals were negative. Colocalization of SSA/Ro52 with autoantigens recognized by murine AAs is seen as yellow in Figure 6.

Exposure to Libby 6-mix resulted in the formation of apoptotic cell surface blebs that were enriched in the SSA/Ro52 autoantigen (Fig. 6A, E and I). AAs from asbestos-exposed mice recognized antigens on the surface of apoptotic cells (Fig. 6C and G) and generated a staining pattern similar to that of SSA/Ro52, indicating a possible colocalization of SSA/Ro52 with the target of asbestos-induced AAs (Arrows in Fig. 6D and H). Conversely, sera from mice exposed to PBS (data not shown) or wollastonite (Fig. 6K) did not recognize apoptotic blebs on the surface of exposed cells. Representative confocal microscopy images are shown in Figure 6. SSA/Ro52 significantly colocalized with AA targets, with a Pearson's correlation coefficient, as determined by Manders and Costes, greater than 0.6 (Fig. 6D and H) (Costes *et al.* 2004; Manders *et al.* 1993). Pearson's correlation coefficient as determined by Manders, Costes' automatic threshold, and Costes' randomization was 0.612, 0.65 and 0.612 for Fig. 6D and 0.704, 0.734 and 0.702 for Fig. 6H, respectively. Thus AAs from mice exposed to Libby 6-mix colocalize with SSA/Ro52 on cell surface blebs of asbestos-induced apoptotic cells.

Discussion

Environmental exposure to crystalline silicates, such as silica and asbestos, generate the production of AAs and induce autoimmune phenotypes in humans and in mice. Exposure to silica exacerbates autoimmune responses in individuals in 'dusty' trades as well as autoimmune prone NZM 2410 mice (Brown 2004; Parks and Cooper 2005). In addition to AA production and disease pathology, silica-exposed NZM mice produce autoantibodies that bind to macrophages undergoing silica-induced apoptosis (Pfau et al. 2004). This disease exacerbated by intratracheal silica is ameliorated by co-instillation with rottlerin, a putative PKC-δ and apoptosis inhibitor (Brown et al. 2005), indirectly supporting a role for apoptosis. Because humans exposed to Libby amphibole asbestos have a significantly higher prevalence of AAs (Pfau et al. 2005), we hypothesized that a similar mechanism might be involved. Therefore, C57Bl/6 mice were intra-tracheally exposed to amphibole asbestos, resulting in the production of AAs including common lupus-associated specificities, anti-SSA/Ro52 and anti-dsDNA (Pfau et al. In Press). This present study sought to determine whether the autoantibodies produced in asbestos exposed mice might elucidate a possible mechanism for asbestos-induced autoimmunity.

Exposure to Libby amphibole asbestos generates an increase in reactive oxygen species and a decrease in intracellular glutathione levels resulting in oxidative stress in murine macrophages (Blake et al. 2007). Libby amphibole asbestos also directly affects human alveolar macrophages leading to an increase in lymphocyte derived cytokine production, which suggests that amphibole asbestos fibers can modify immune function by altering antigen presenting cell (APC) activity (Hamilton et al. 2004). Increased APC activity due to asbestos exposure may up-regulate the normal lymphocyte response to antigens in the lung leading to a loss of tolerance. We hypothesize that asbestos-induced autoimmunity is generated through a “two hit” mechanism. First, autoantigens become visible to the immune system during apoptosis, which results in the accumulation of autoantigens on the cell surface. The subsequent uptake and processing of apoptotic cells by antigen-presenting cells in a pro-inflammatory context will activate self-reactive T cells, inducing the loss of tolerance and generate the autoimmune responses observed in humans and mice.

Cellular antigens targeted by AAs are diverse in terms of their localization, structure and function. However, one common factor among many autoantigens, is that they are enriched in cell surface blebs of apoptotic cells (Casciola-Rosen et al. 1994). The present study indicates that Libby 6-mix asbestos induces apoptosis in macrophages as determined by extracellular PS exposure as measured by Annexin V (Fig. 1). To confirm that apoptosis occurs in response to Libby asbestos exposure, the cleavage of PARP was quantified through immuoblotting. Cleavage of full length PARP after exposure to Libby asbestos was evident after 24 h and was associated with an increase in the cleaved fragment of PARP after 48 and 72 h (Fig. 2). Finally, exposure to Libby 6-mix asbestos induces morphological changes in macrophages, such as nuclear condensation and cell surface blebbing, which is another well characterized feature of apoptosis (Nozawa et al. 2002).

The cell surface blebs, generated by asbestos-induced apoptosis, are enriched in the SSA/Ro52 autoantigen (Fig. 4H and L). However, murine macrophages were not permeabilized prior to staining though the nuclei of all cells stained with PI. Therefore, PI staining of unpermeabilized cells may be an artifact of the fixation process, possibly by causing minor permeabilization in the plasma membrane. Membrane permeabilization may be of concern if the staining of SSA/Ro52 surface blebs were due to the leakage of the plasma membrane. However, our data clearly indicate that the SSA autoantigen was retained within intact cell surface membrane blebs as shown by Figure 4 and was verified by Z-stack analysis. These cell surface blebs may be the potential stimuli for the initiation of an autoimmune response. Indeed, murine AAs from asbestos exposed mice recognize SSA/Ro52 on the surface of apoptotic macrophages indicating the antigenicity of SSA/Ro52 (Fig. 6D and H).

The binding of AAs to apoptotic cells has been previously shown to inhibit clearance leading to the accumulation of apoptotic cells, which can promote inflammation and tissue damage (Clancy *et al.* 2006; Gandhi *et al.* 2006; Salomonsson *et al.* 2005). Therefore, AAs induced by asbestos may exacerbate tissue damage in the lung, further promoting inflammation and fibrosis. Indeed, positive correlations were found between ANA titers and lung disease severity and extent of exposure in serum samples from the Libby cohort, indicating that autoantibodies are associated with asbestos-related diseases (ARD) (Pfau et al. 2005). Interestingly, similar to mice exposed to amphibole asbestos, resident from Libby also generate anti-SSA/Ro52 autoantibodies (unpublished results). However, the exact role of anti-SSA/Ro52 autoantibodies in the development or progression of ARD has not been elucidated.

Other apoptosis-inducing stimuli, such as UV radiation, TNF-alpha and staurosporine, have been shown to induce the blebbing of SSA/Ro52 to the cell surface (Casciola-Rosen et al. 1994; McArthur et al. 2002; Ohlsson et al. 2002; Saegusa et al. 2002), however not all xenobiotics induce the production of anti-SSA/Ro52 autoantibodies. Because apoptosis alone

does not elicit autoimmunity, a second pro-inflammatory signal such as an adjuvant must be provided in order to generate an immune response (Bondanza *et al.* 2004; Mevorach *et al.* 1998; Tzeng *et al.* 2006). Asbestos induces a highly inflammatory state in the lung (Fattman *et al.* 2006; Kamp and Weitzman 1999; Tan *et al.* 2004). Moreover, exposure to amphibole asbestos in alveolar macrophages has been previously shown to increase the release of pro-inflammatory cytokines such as TNF-α and IL-1 (Driscoll et al. 1995). In this pro-inflammatory environment an increase in apoptosis may lead to excess presentation of autoantigens thereby exacerbating an autoimmune response.

In summary, exposure to Libby amphibole asbestos induces apoptosis in murine macrophages which results in the formation of cell surface blebs enriched in the SSA/Ro52 autoantigen. These apoptotic blebs containing SSA/Ro52 are recognized by AAs from asbestos exposed mice. This study provides further compelling evidence for the role of apoptosis in the induction of xenobiotic autoimmune responses by demonstrating the translocation of an autoantigen to apoptotic material following asbestos exposure.

Acknowledgements

The authors thank Sheng'ai Li, University of Montana, for helpful discussions and technical assistance, Pamela Shaw in the CEHS Fluorescence Cytometry Core for assistance with the FACS analysis and Lou Herritt in the CEHS Histology and Imaging Core for assistance with the confocal microscopy analysis.

Grants This work was funded by grants from the NIH COBRE P20 NCRR017670, R21 ES012956 and from the University of Montana Graduate School.

References

Blake DJ, Bolin CM, Cox DP, Cardozo-Pelaez F, Pfau JC. Internalization of Libby amphibole asbestos and induction of oxidative stress in murine macrophages. Toxicological Sciences 2007;99:277–288. [PubMed: 17578862]

Bolte S, Cordelieres FP. A guided tour into subcellular colocalization analysis in light microscopy. J Microsc 2006;224:213–232. [PubMed: 17210054]

Bondanza A, Zimmermann VS, Dell'Antonio G, Cin ED, Balestrieri G, Tincani A, Amoura Z, Piette JC, Sabbadini MG, Rovere-Querini P, Manfredi AA. Requirement of dying cells and environmental adjuvants for the induction of autoimmunity. Arthritis Rheum 2004;50:1549–1560. [PubMed: 15146425]

Brown JM, Pfau JC, Pershouse MA, Holian A. Silica, Apoptosis and Autoimmunity. Journal of Immunotoxicology 2004;1:177–187. [PubMed: 18958651]

Brown JM, Schwanke CM, Pershouse MA, Pfau JC, Holian A. Effects of rottlerin on silica-exacerbated systemic autoimmune disease in New Zealand mixed mice. Am J Physiol Lung Cell Mol Physiol 2005;289:L990–L998. [PubMed: 16040631]

Casciola-Rosen LA, Anhalt G, Rosen A. Autoantigens targeted in systemic lupus erythematosus are clustered in two populations of surface structures on apoptotic keratinocytes. J Exp Med 1994;179:1317–1330. [PubMed: 7511686]

Casiano CA, Martin SJ, Green DR, Tan EM. Selective cleavage of nuclear autoantigens during CD95 (Fas/APO-1)-mediated T cell apoptosis. J Exp Med 1996;184:765–770. [PubMed: 8760832]

Clancy RM, Neufing PJ, Zheng P, O'Mahony M, Nimmerjahn F, Gordon TP, Buyon JP. Impaired clearance of apoptotic cardiocytes is linked to anti-SSA/Ro and -SSB/La antibodies in the pathogenesis of congenital heart block. J Clin Invest 2006;116:2413–2422. [PubMed: 16906225]

Costes SV, Daelemans D, Cho EH, Dobbin Z, Pavlakis G, Lockett S. Automatic and quantitative measurement of protein-protein colocalization in live cells. Biophys J 2004;86:3993–4003. [PubMed: 15189895]

D'Cruz D. Autoimmune diseases associated with drugs, chemicals and environmental factors. Toxicol Lett 2000;112–113:421–432.

Driscoll KE, Maurer JK, Higgins J, Poynter J. Alveolar macrophage cytokine and growth factor production in a rat model of crocidolite-induced pulmonary inflammation and fibrosis. J Toxicol Environ Health 1995;46:155–169. [PubMed: 7563215]

Duriez PJ, Shah GM. Cleavage of poly(ADP-ribose) polymerase: a sensitive parameter to study cell death. Biochem Cell Biol 1997;75:337–349. [PubMed: 9493956]

Espinosa A, Zhou W, Ek M, Hedlund M, Brauner S, Popovic K, Horvath L, Wallerskog T, Oukka M, Nyberg F, Kuchroo VK, Wahren-Herlenius M. The Sjogren's syndrome-associated autoantigen Ro52 is an E3 ligase that regulates proliferation and cell death. J Immunol 2006;176:6277–6285. [PubMed: 16670339]

Fattman CL, Tan RJ, Tobolewski JM, Oury TD. Increased sensitivity to asbestos-induced lung injury in mice lacking extracellular superoxide dismutase. Free Radic Biol Med 2006;40:601–607. [PubMed: 16458190]

Gandhi R, Hussain E, Das J, Handa R, Pal R. Anti-idiotype-mediated epitope spreading and diminished phagocytosis by a human monoclonal antibody recognizing late-stage apoptotic cells. Cell Death Differ 2006;13:1715–1726. [PubMed: 16470225]

Hamilton RF, Iyer LL, Holian A. Asbestos induces apoptosis in human alveolar macrophages. Am J Physiol 1996;271:L813–L819. [PubMed: 8944725]

Hamilton RF Jr, Holian A, Morandi MT. A comparison of asbestos and urban particulate matter in the in vitro modification of human alveolar macrophage antigen-presenting cell function. Exp Lung Res 2004;30:147–162. [PubMed: 14972774]

Hassan AB, Lundberg IE, Isenberg D, Wahren-Herlenius M. Serial analysis of Ro/SSA and La/SSB antibody levels and correlation with clinical disease activity in patients with systemic lupus erythematosus. Scand J Rheumatol 2002;31:133–139. [PubMed: 12195626]

Hess EV. Environmental chemicals and autoimmune disease: cause and effect. Toxicology 2002;181–182:65–70.

Hoffman IE, Peene I, Meheus L, Huizinga TW, Cebecauer L, Isenberg D, De Bosschere K, Hulstaert F, Veys EM, De Keyser F. Specific antinuclear antibodies are associated with clinical features in systemic lupus erythematosus. Ann Rheum Dis 2004;63:1155–1158. [PubMed: 15308527]

Igarashi T, Itoh Y, Fukunaga Y, Yamamoto M. Stress-induced cell surface expression and antigenic alteration of the Ro/SSA autoantigen. Autoimmunity 1995;22:33–42. [PubMed: 8882420]

Kamp DW, Weitzman SA. The molecular basis of asbestos induced lung injury. Thorax 1999;54:638–652. [PubMed: 10377212]

Manders EMM, Verbeek FJ, Aten JA. Measurement of co-localisation of objects in dual-colour confocal images. J. Microsc 1993;169:375–382.

McArthur C, Wang Y, Veno P, Zhang J, Fiorella R. Intracellular trafficking and surface expression of SS-A (Ro), SS-B (La), poly(ADP-ribose) polymerase and alpha-fodrin autoantigens during apoptosis in human salivary gland cells induced by tumour necrosis factor-alpha. Arch Oral Biol 2002;47:443–448. [PubMed: 12102760]

Mevorach D, Zhou JL, Song X, Elkon KB. Systemic exposure to irradiated apoptotic cells induces autoantibody production. J Exp Med 1998;188:387–392. [PubMed: 9670050]

Miranda ME, Tseng CE, Rashbaum W, Ochs RL, Casiano CA, Di Donato F, Chan EK, Buyon JP. Accessibility of SSA/Ro and SSB/La antigens to maternal autoantibodies in apoptotic human fetal cardiac myocytes. J Immunol 1998;161:5061–5069. [PubMed: 9794444]

Noonan CW, Pfau JC, Larson TC, Spence MR. Nested case-control study of autoimmune disease in an asbestos-exposed population. Environ Health Perspect 2006;114:1243–1247. [PubMed: 16882533]

Nozawa K, Casiano CA, Hamel JC, Molinaro C, Fritzler MJ, Chan EK. Fragmentation of Golgi complex and Golgi autoantigens during apoptosis and necrosis. Arthritis Res 2002;4:R3. [PubMed: 12106502]

Ohlsson M, Jonsson R, Brokstad KA. Subcellular redistribution and surface exposure of the Ro52, Ro60 and La48 autoantigens during apoptosis in human ductal epithelial cells: a possible mechanism in the pathogenesis of Sjogren's syndrome. Scand J Immunol 2002;56:456–469. [PubMed: 12410795]

Parks CG, Cooper GS. Occupational exposures and risk of systemic lupus erythematosus. Autoimmunity 2005;38:497–506. [PubMed: 16373255]

Pfau JC, Brown JM, Holian A. Silica-exposed mice generate autoantibodies to apoptotic cells. Toxicology 2004;195:167–176. [PubMed: 14751672]

Pfau JC, Sentissi JJ, Blake DJ, Li S, Calderon-Garciduenas L, Brown JM. Asbestos-Induced Autoimmunity in C57Bl/6 Mice. Journal of Immunotoxicology. In Press

Pfau JC, Sentissi JJ, Weller G, Putnam EA. Assessment of autoimmune responses associated with asbestos exposure in Libby, Montana, USA. Environ Health Perspect 2005;113:25–30. [PubMed: 15626643]

Popovic K, Brauner S, Ek M, Wahren-Herlenius M, Nyberg F. Fine specificity of the Ro/SSA autoantibody response in relation to serological and clinical findings in 96 patients with self-reported cutaneous symptoms induced by the sun. Lupus 2007;16:10–17. [PubMed: 17283579]

Rosen A, Casciola-Rosen L. Autoantigens as substrates for apoptotic proteases: implications for the pathogenesis of systemic autoimmune disease. Cell Death Differ 1999;6:6–12. [PubMed: 10200542]

Rosen A, Casciola-Rosen L. Altered autoantigen structure in Sjogren's syndrome: implications for the pathogenesis of autoimmune tissue damage. Crit Rev Oral Biol Med 2004;15:156–164. [PubMed: 15187033]

Routsias JG, Vlachoyiannopoulos PG, Tzioufas AG. Autoantibodies to intracellular autoantigens and their B-cell epitopes: molecular probes to study the autoimmune response. Crit Rev Clin Lab Sci 2006;43:203–248. [PubMed: 16574554]

Saegusa J, Kawano S, Koshiba M, Hayashi N, Kosaka H, Funasaka Y, Kumagai S. Oxidative stress mediates cell surface expression of SS-A/Ro antigen on keratinocytes. Free Radic Biol Med 2002;32:1006–1016. [PubMed: 12008116]

Salomonsson S, Sonesson SE, Ottosson L, Muhallab S, Olsson T, Sunnerhagen M, Kuchroo VK, Thoren P, Herlenius E, Wahren-Herlenius M. Ro/SSA autoantibodies directly bind cardiomyocytes, disturb calcium homeostasis, and mediate congenital heart block. J Exp Med 2005;201:11–17. [PubMed: 15630133]

Tan RJ, Fattman CL, Watkins SC, Oury TD. Redistribution of pulmonary EC-SOD after exposure to asbestos. J Appl Physiol 2004;97:2006–2013. [PubMed: 15298984]

Tzeng TC, Suen JL, Chiang BL. Dendritic cells pulsed with apoptotic cells activate self-reactive T-cells of lupus mice both in vitro and in vivo. Rheumatology (Oxford) 2006;45:1230–1237. [PubMed: 16595513]

van Engeland M, Ramaekers FC, Schutte B, Reutelingsperger CP. A novel assay to measure loss of plasma membrane asymmetry during apoptosis of adherent cells in culture. Cytometry 1996;24:131–139. [PubMed: 8725662]

Wada K, Kamitani T. Autoantigen Ro52 is an E3 ubiquitin ligase. Biochem Biophys Res Commun 2006;339:415–421. [PubMed: 16297862]

Xia T, Kovochich M, Brant J, Hotze M, Sempf J, Oberley T, Sioutas C, Yeh JI, Wiesner MR, Nel AE. Comparison of the abilities of ambient and manufactured nanoparticles to induce cellular toxicity according to an oxidative stress paradigm. Nano Lett 2006;6:1794–1807. [PubMed: 16895376]

Yamaki K, Hong J, Hiraizumi K, Ahn JW, Zee O, Ohuchi K. Participation of various kinases in staurosporine induced apoptosis of RAW 264.7 cells. J Pharm Pharmacol 2002;54:1535–1544. [PubMed: 12495557]

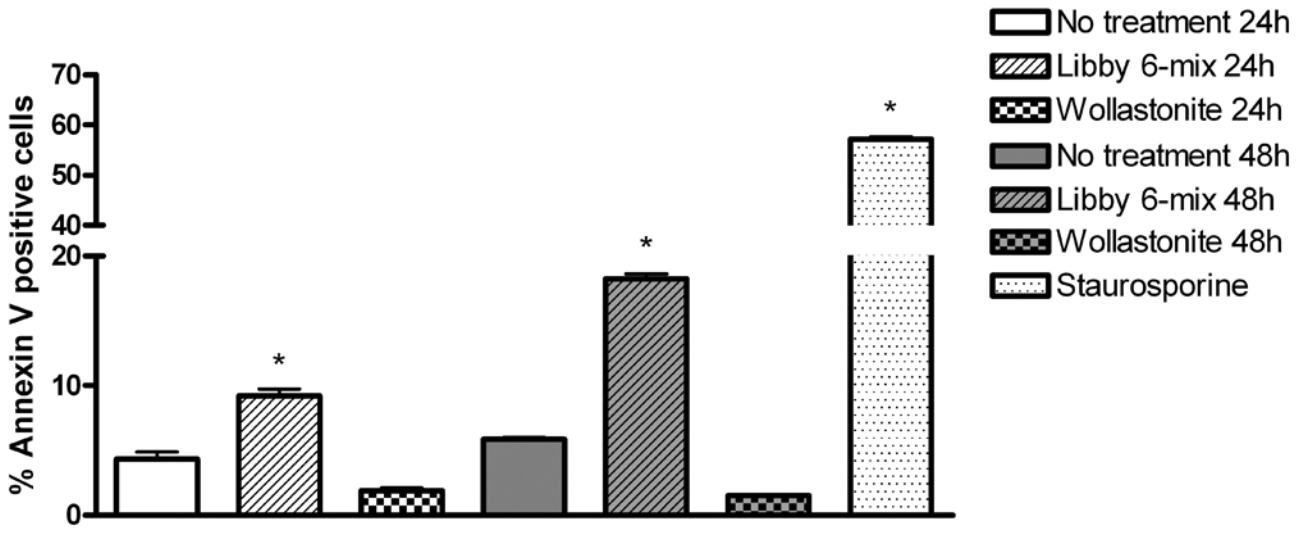

Figure 1.

Libby 6-mix induces apoptosis in murine macrophages. RAW264.7 cells were exposed to Libby amphibole asbestos or wollastonite fibers (62.5 μg/cm^2) for 72 h or 1 μM staurosporine for 6 h. Apoptosis was quantified through Annexin V staining as described in Materials and Methods. Apoptosis was quantified as the percent of cells that were positive for Annexin V staining through flow cytometry. Results represent mean percentages ± SEM from two independent experiments. Asterisks indicate a significant increase compared to time matched controls ($P < 0.05$, $n = 3$).

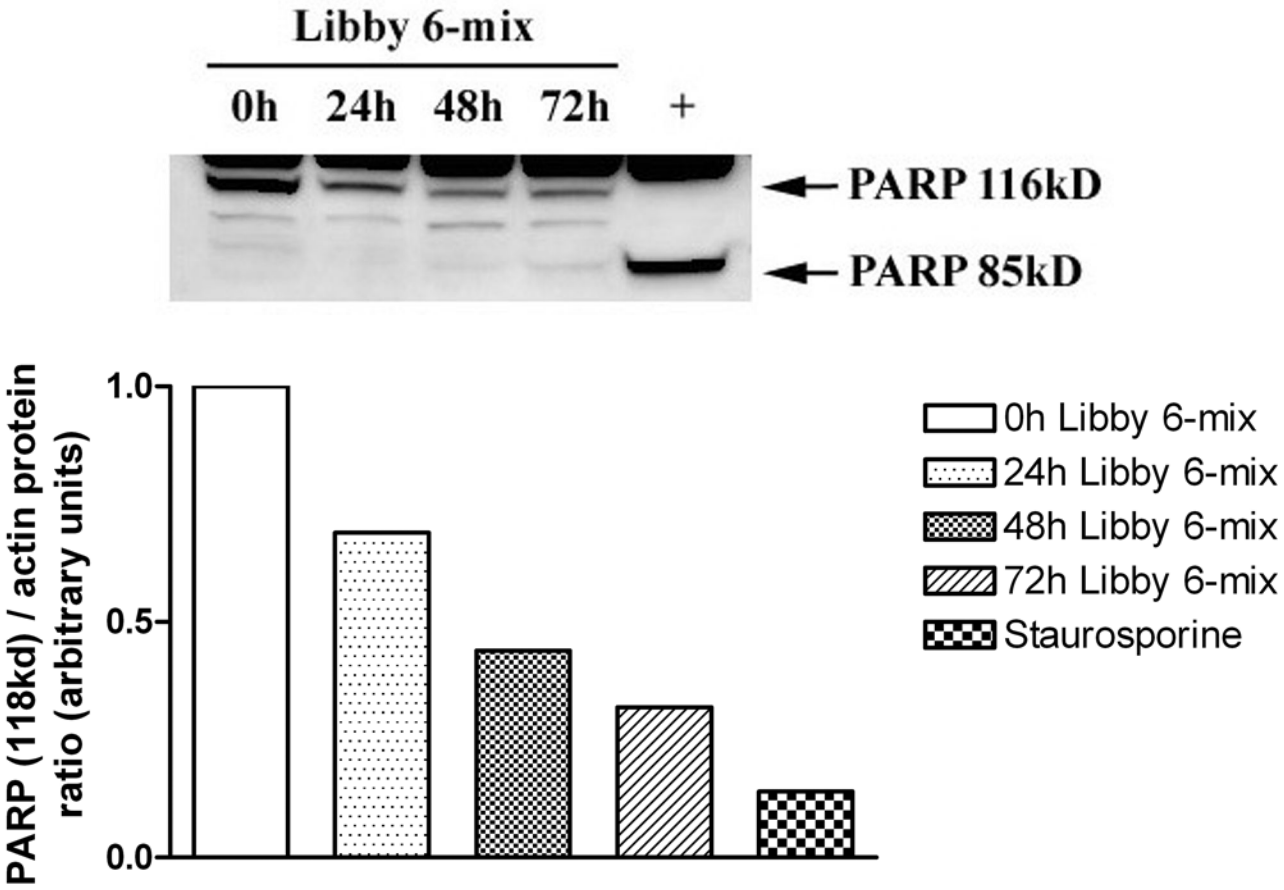

Figure 2.

Libby 6-mix exposure results in the cleavage of PARP. A) RAW264.7 cells were exposed to Libby 6-mix fibers at a final concentration of 62.5 μg/cm^2 for 72 h or to 1 μM staurosporine for 6 h (positive control). Cell lysates were prepared and analyzed through immunoblotting using an anti-PARP rabbit polyclonal that detects the full length protein (116 kDa) and the cleaved fragment (85 kDa). B) Quantification of full length PARP from RAW264.7 cells exposed to Libby 6-mix. Values signify the densitometric units determined for the immunoreactive bands of full length PARP divided by the densitometric units determined for the immunoreactive bands of the actin loading control and reported as the fold change compared to control.

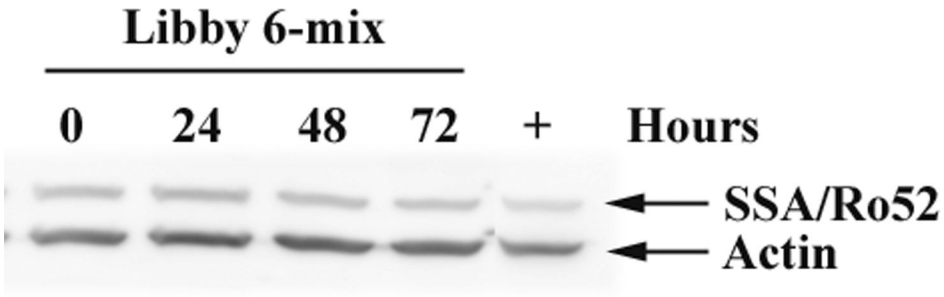

Figure 3.
The SSA/Ro52 autoantigen is not cleaved during apoptosis. RAW264.7 cells were exposed to Libby 6-mix fibers at a final concentration of 62.5 μg/cm^2 for 72 h or to 1 μM staurosporine for 6 h (positive control). Cell lysates were prepared and analyzed through immunoblotting using an anti-SSA/Ro52 rabbit polyclonal antibody and an antiactin rabbit polyclonal antibody.

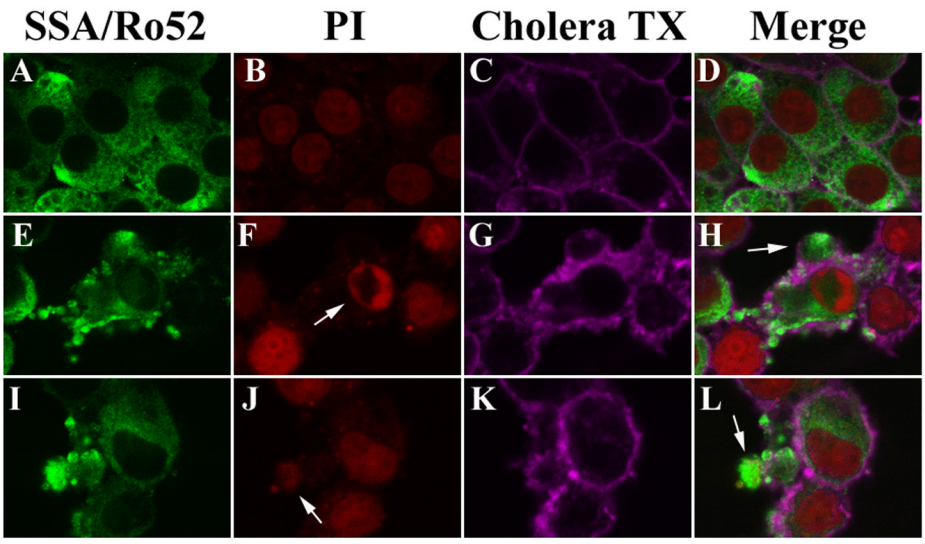

Figure 4.

Libby 6-mix exposure results in the redistribution of SSA/Ro52 to surface blebs of apoptotic cells. Representative confocal microcopy images of RAW264.7 cells untreated (Panels A–D) or exposed to Libby asbestos for 48 h (Panels E–L). The distribution of the SSA/Ro52 autoantigen was visualized through confocal microscopy using a rabbit polyclonal anti-SSA/Ro52 and an Alexa Fluor 488 conjugated goat anti-rabbit IgG secondary (Green in panels A, E and I). Nuclei were counterstained with propidium iodide (Red in panels B, F and J). Apoptotic nuclei are indicated by arrows. The plasma membrane was visualized with Alexa Fluor 647 cholera toxin subunit B conjugate (Magenta in panels C, G and K). Right panels (D, H and L) show merged images with arrows indicating apoptotic cell surface blebs enriched in SSA/Ro52.

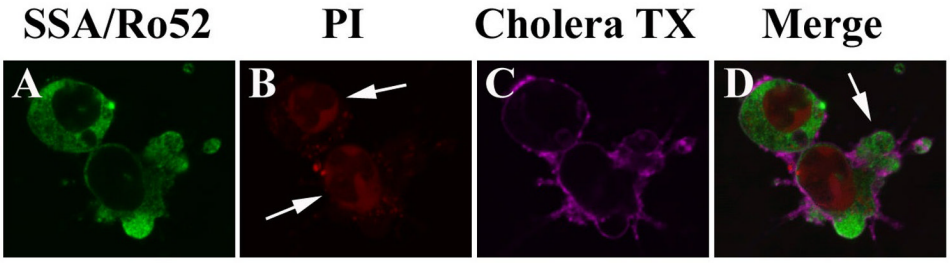

Figure 5.

Staurosporine treatment results in the redistribution of SSA/Ro52 to surface blebs of apoptotic cells. A representative confocal microcopy image of RAW264.7 cells treated with 1 μM staurosporine for 6 h. The distribution of the SSA/Ro52 autoantigen was visualized through confocal microscopy using a rabbit polyclonal anti-SSA/Ro52 and an Alexa Fluor 488 conjugated goat anti-rabbit IgG secondary (Panel A). Nuclei were counterstained with propidium iodide (Panel B). Apoptotic nuclei are indicated by arrows. The plasma membrane was visualized with Alexa Fluor 647 cholera toxin subunit B conjugate (Panel C). Panel D shows the merged image with an arrow indicating apoptotic cell surface blebs enriched in SSA/Ro52.

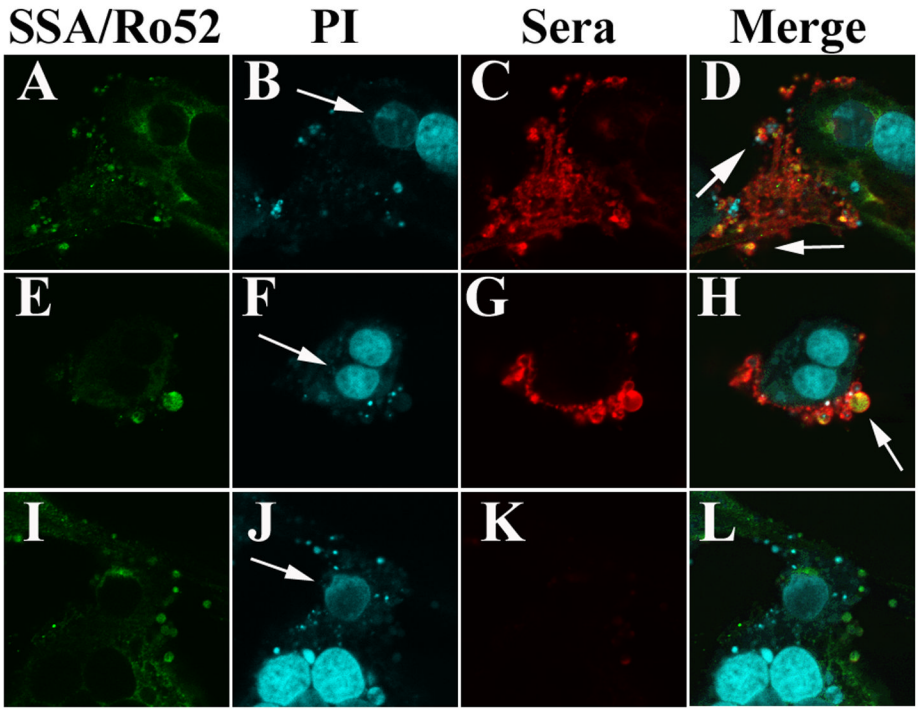

Figure 6.

Autoantibodies from asbestos-exposed mice recognize apoptotic blebs enriched with the SSA/Ro52 autoantigen. Representative confocal microcopy images of RAW264.7 cells exposed to Libby asbestos for 48 h. The SSA/Ro52 autoantigen was visualized through confocal microscopy using a rabbit polyclonal anti-SSA/Ro52 antibody and an Alexa Fluor 488 conjugated goat anti-rabbit IgG secondary (Green in panels A, E and I). Nuclei were counterstained with propidium iodide (Cyan in panels B, F and J). Apoptotic nuclei are indicated by arrows. Binding of mouse autoantibodies were visualized with an Alexa Fluor 647 conjugated goat anti-mouse IgG secondary (Red in panels C, G and K). Panels C and G include AA staining from a mouse exposed to tremolite asbestos. Panel K includes AA staining from a mouse exposed to wollastonite fibers. Right panels (D, H and L) show merged images. Colocalization of SSA/Ro52 and autoantigens recognized by asbestos-induced mouse AAs is visualized in yellow in merged images and indicated by arrows. Colocalization was confirmed through Image J analysis.